

DIAMOND-CLEANING INVESTIGATIONS

T E Derry

NUCLEAR PHYSICS RESEARCH UNIT
UNIVERSITY OF THE WITWATERSRAND
1 JAN SMUTS AVENUE
JOHANNESBURG
2001

APR 77/3

ISBN 0 85494 435 4

DIAMOND-CLEANING INVESTIGATIONS.

INTRODUCTION

This investigation was undertaken by the Witwatersrand University Nuclear Physics Research Unit in collaboration with Professor R. Ditchburn and the Diamond Research Laboratories to examine the efficacy of cleaning gem diamonds using our methods for producing very clean surfaces for ion beam experiments.

De Beers supplied 4 parcels of diamonds which either had or had not been cleaned using their usual techniques, chiefly involving an etch in molten potassium nitrate. Each parcel contained about 40 stones, amounting to about 10 carats (see Table 1). Half of the diamonds in each parcel were cleaned by our standard procedure : $\frac{1}{2}$ hour's ultrasonic agitation in a 20% solution of the commercial detergent 'Contrad' (sold as 'Decon 90' in some countries). The chief ingredients of this are believed to be a surfactant and a chelating agent.

Visual comparisons of different groups of stones by a number of observers who were not told the stones' histories, established that the diamonds generally had a more sparkling appearance after our cleaning procedure had been applied.

NUCLEAR ANALYSIS

Our work is more concerned with monitoring impurities on an atomic scale using the large-angle Rutherford scattering of accelerated helium ions. The ion beam is directed at the surface of a diamond in vacuum, and backscattered particles detected at 155° by a surface-

barrier detector, which produces electronic pulses of a height proportional to the particles' energy. Using standard nuclear electronics, an energy spectrum (number of particles vs. energy) is plotted .

When an ion of energy E_0 and mass M_1 collides with an atom of mass M_2 and is scattered through an angle θ , its emergent energy is

$$E = \left\{ \frac{M_1 \cos \theta}{M_1 + M_2} + \sqrt{\left(\frac{M_1 \cos \theta}{M_1 + M_2} \right)^2 + \frac{M_2 - M_1}{M_1 + M_2}} \right\}^2 E_0$$

Thus the energies of ions, of fixed incident energy, backscattered from a thin layer of solid (e.g. an impurity layer on diamond) depend only on the mass or masses of the atoms in the layer. Each impurity element results in a peak in the energy spectrum, from the position of which the mass can be deduced. The number of counts in the peak is proportional to the number of impurity atoms present; the peak width is due to instrumental factors.

If the solid is present in bulk rather than in a thin layer, then the peak spreads to lower energies and becomes a plateau with a well-defined high energy edge. This results from the slowing-down of ions as they penetrate: ions which were scattered at greater and greater depths are detected with progressively lower energies. The spectrum of the diamond itself is of this type.

EXPERIMENTAL

One representative stone was selected from each parcel and a spectrum taken with 1 MeV helium ions provided by the pressurized Cockcroft-Walton accelerator in the Nuclear Physics Research Unit. Another

spectrum was taken after cleaning in 'Contrad'.

The mass resolution of these spectra varies across the spectral energy range, being roughly ± 1 mass unit in the middle region ($20 < M < 60$), less at lower energies, and greater than 1u for greater energies and masses.

RESULTS : CLEAR STONES

The contents of parcels 4,6, and 7 were all similar in appearance, being clear stones with many good octahedra. The 'uncleaned' spectra too were quite similar, showing little impurity irrespective of whether the stones had been precleaned using fused KNO_3 , as had parcel 4. This can be seen in figures 1(a), 2(a), and 3(a). Apart from the carbon ($M = 12$) plateau referred to above, and a peak due to oxygen ($M = 16$) which is always present on diamond surfaces at about the monolayer level there is in each case a small peak at $M = 41$ (or 40), corresponding to calcium. The reason for its presence is not obvious. All stones show a distribution of other mass-numbers, notably the sample from parcel 6.

In all cases, the stones show even lower impurity levels after Contrad cleaning (figs. 1(b), 2(b), and 3(b)). For instrumental reasons, the vertical scales on the (a) and (b) figures are slightly different, but can be judged by the height of the carbon plateau. The greatest improvement is in the dirtiest stone (No. 6); the calcium impurity on all stones has been reduced or eliminated. The residual counts are at a level probably due mainly to unwanted multiple scattering in the apparatus. The least improvement is in the stone given the KNO_3 pretreatment (No. 4), and it seems to have

increased, or at least retained, some high-mass contamination. A peak on No. 7 at $M=58$ is probably due to iron ($M = 56$) and may have rubbed off from the steel sample-holder during mounting.

RED-STAINED STONES

Parcel No. 11 contained stones of a quite different appearance to the others, marbled with red veins thought to be due to the oxidation of abundant iron-bearing contamination to Fe_2O_3 by the KNO_3 process. The presence of iron was confirmed by positioning the beam-spot on one of the red stains and taking a spectrum (fig.4). However, other impurities are present in even greater concentrations: oxygen, silicon, chlorine and calcium (or potassium), with traces of heavier elements. Since the spectrum shows plateaus rather than peaks, all are present in thick layers, or are distributed into the crystal. The Rutherford cross-section is proportional to the square of the atomic number, so division of counts per channel for each element by Z^2 gives the relative atomic abundances (see table, fig. 4). However, one cannot use these figures to work out a 'formula' for the contaminant, since several compounds are almost certainly involved. The major one is probably silica.

The beam was also directed at an apparently plain area of the crystal, and at a red 'interface' (perhaps a filled microcrack). Both areas show similar heavy contamination, although less than the red stain (figs. 6(a) and 7(a)). Elements present probably include ^{16}O , ^{28}Si , ^{40}Ca (or ^{45}Sc), ^{56}Fe , ^{63}Cu , and ^{208}Pb .

Contrad cleaning was unable to remove completely this heavy contamination, but made considerable improvement (see figs. 5(b),

6(b), and 7(b)). Peaks of resistant contamination - notably oxygen, silicon and copper, plus calcium and iron in the red-stain region - now stand up above a cleaner background. There was no visible reduction in the density of the red stains. It is interesting that the opposite side of No. 11 was as clean as stones from the other three parcels.

CONCLUSION

Using a sensitive nuclear method, we can demonstrate the effectiveness of diamond-cleaning procedures. Our method using a commercial detergent appears to make a greater improvement to an uncleaned stone than the fused potassium-nitrate method, even for heavily contaminated samples. The elemental composition of contaminants can be determined, if required.

TABLE 1

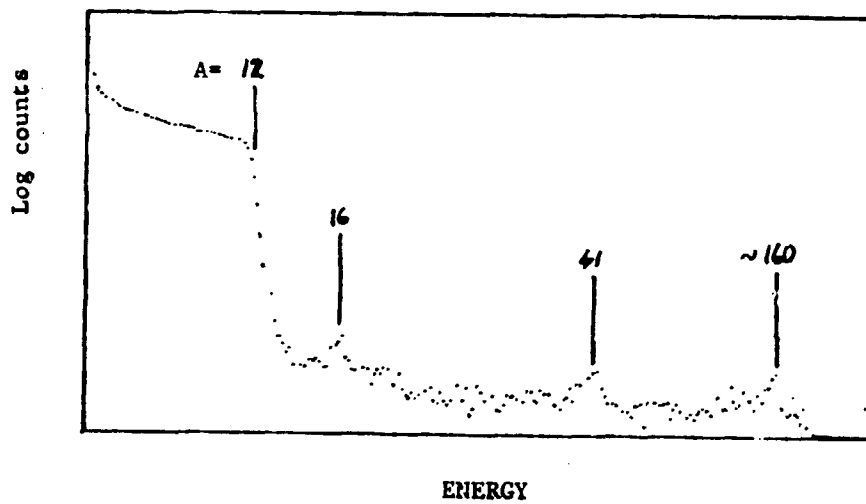
List of diamond packets

Packet Number	No. of stones	Carats	Description
4	44	10,1	Cleaned by Mr Bark in London with KNO_3
6	46	10,1	Uncleaned
7	43	10,1	Uncleaned
11	35	16,7	Red-stained

FIG. 1

PARCEL 4 (pretreated with KNO_3)

(a) before cleaning



(b) after cleaning

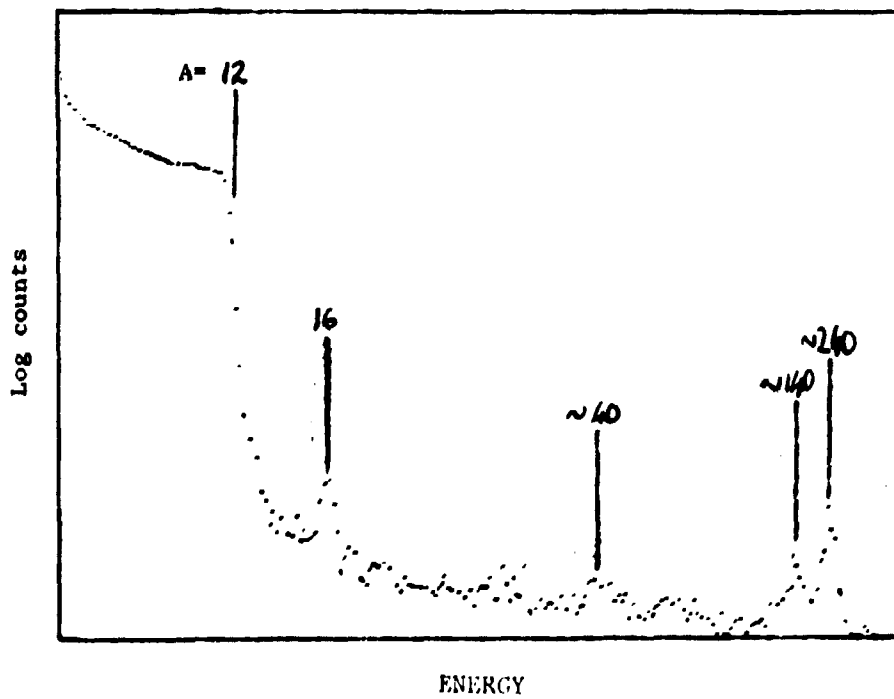
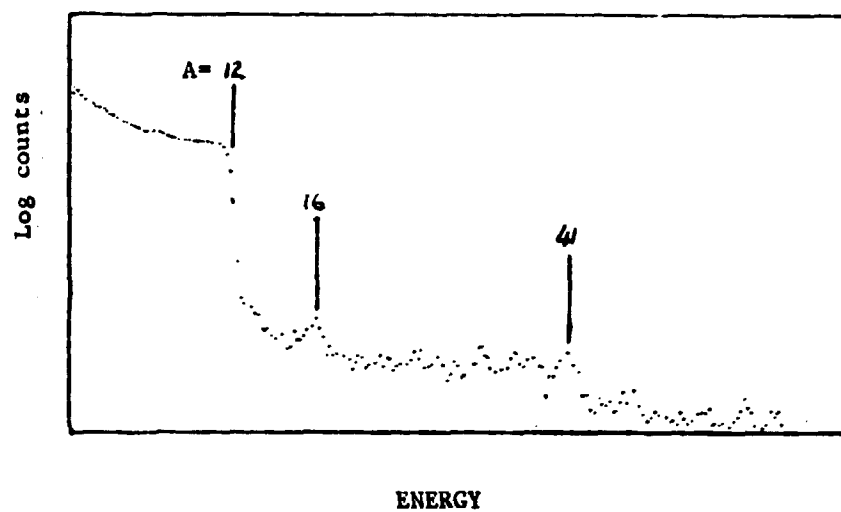


FIG. 2

PARCEL 6 (no pretreatment)

(a) before cleaning



(b) after cleaning

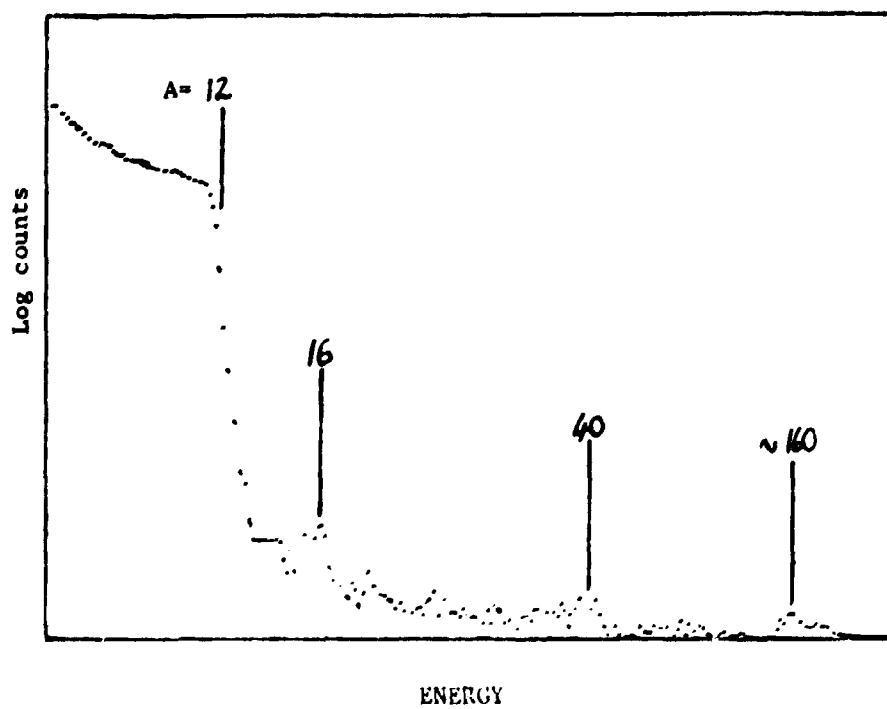
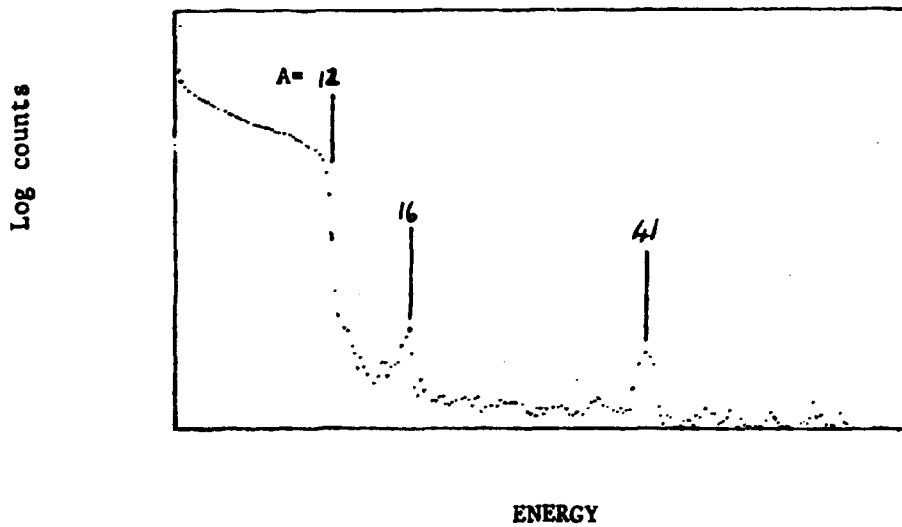


FIG. 3

PARCEL 7 (no pretreatment)

(a) before cleaning



(b) after cleaning

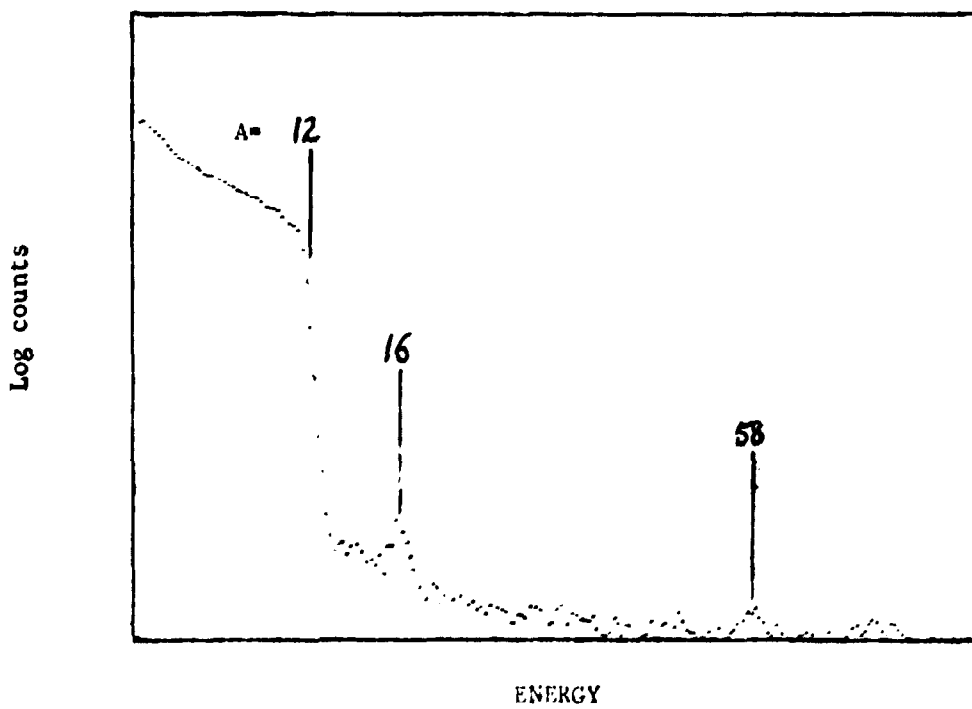


FIG. 4

PARCEL 11 (red-stained)

Region (i) : red stain. Before cleaning

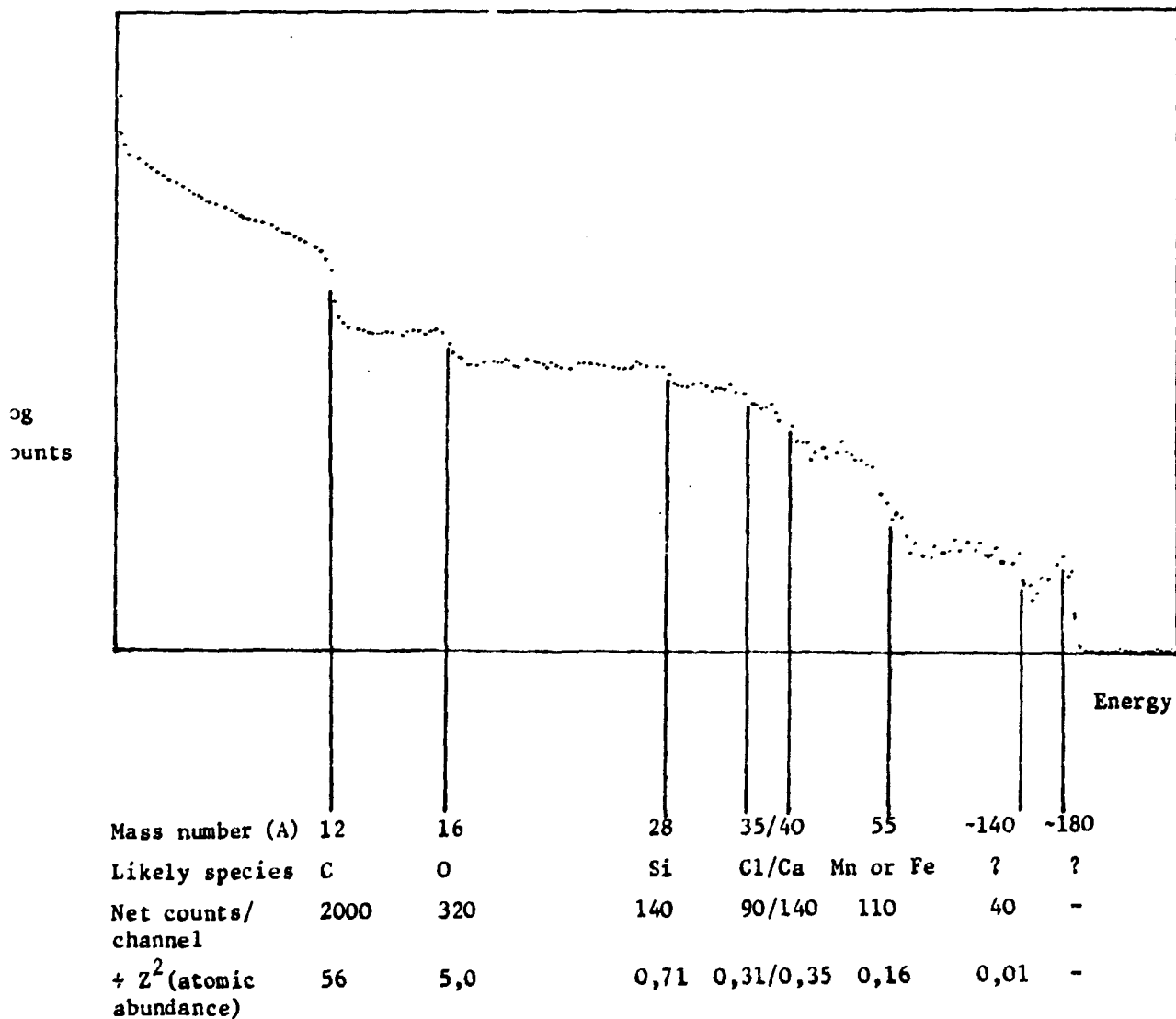
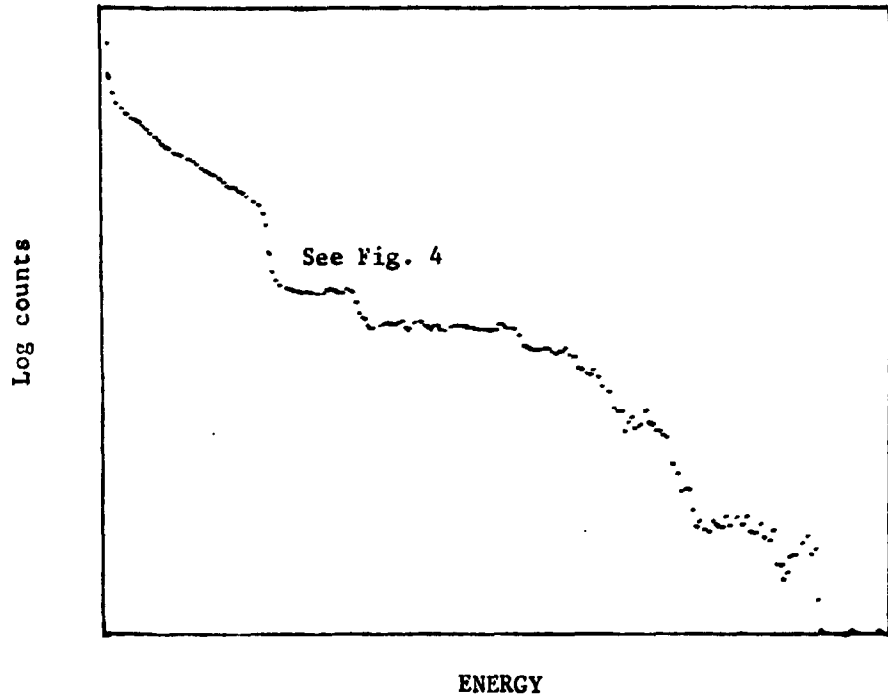


FIG. 5

PARCEL 11 (red-stained)

Region (i) : red stain.

(a) Before cleaning



(b) After cleaning

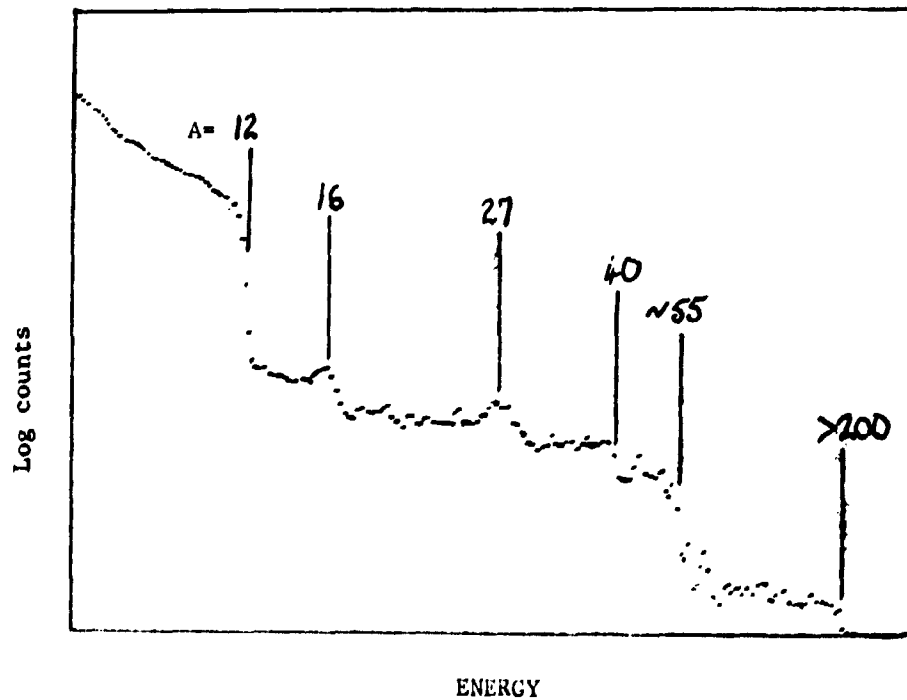
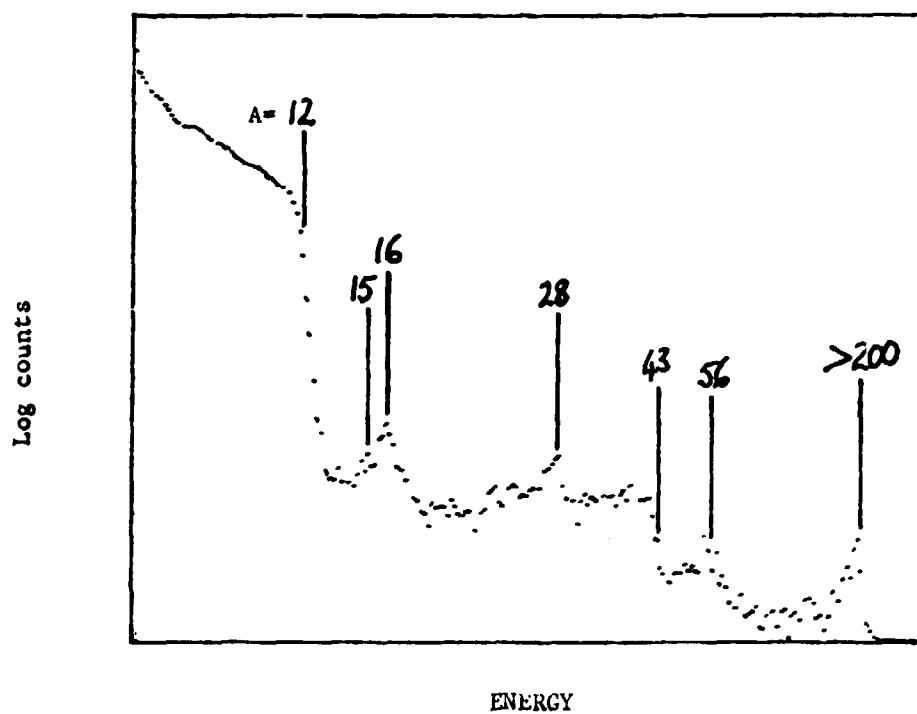


FIG. 6

PARCEL 11 (red-stained)

Region (ii) : plain area

(a) Before cleaning



(b) After cleaning

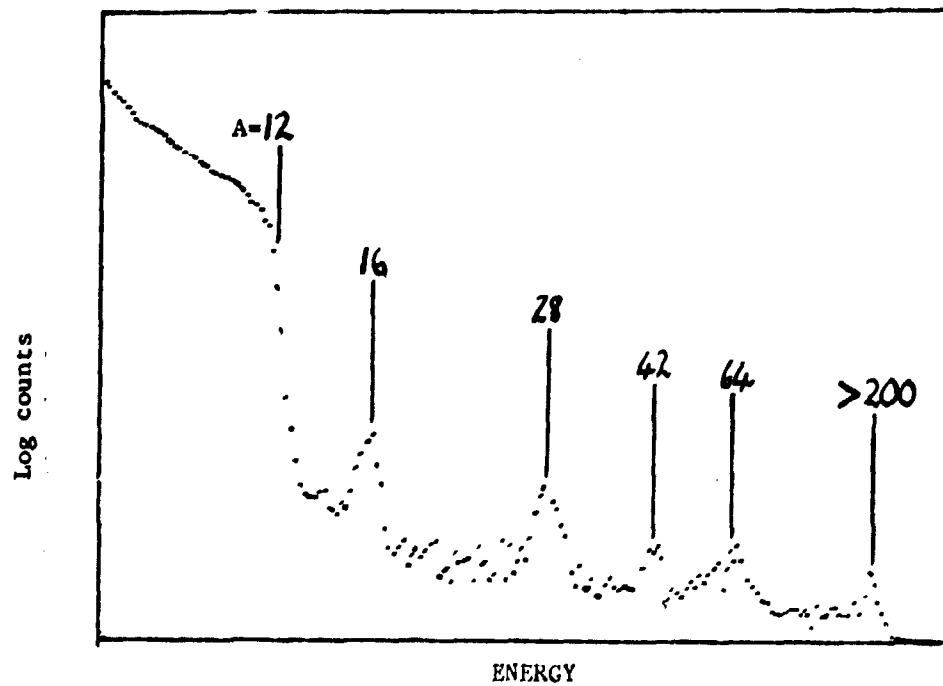
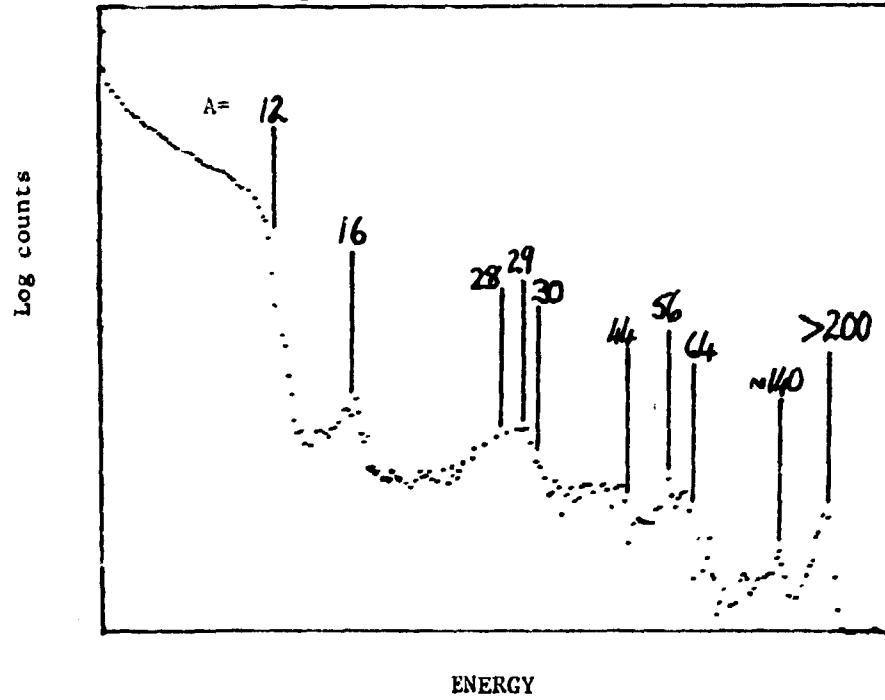


FIG. 7

PARCEL 11 (red-stained)

Region (iii) : red interface

(a) before cleaning



(b) after cleaning

